

Confronting Spectral Functions from e^+e^- Annihilation and τ Decays: Consequences for the Muon Magnetic Moment

A. Höcker^{a*},

^aLaboratoire de l'Accélérateur Linéaire,
IN2P3-CNRS et Université de Paris-Sud, F-91898 Orsay, France
(e-mail: hoecker@lal.in2p3.fr)

Vacuum polarization integrals involve the vector spectral functions which can be experimentally determined from two sources: (i) e^+e^- annihilation cross sections and (ii) hadronic τ decays. Recently results with comparable precision have become available from CMD-2 on one side, and ALEPH, CLEO and OPAL on the other. The comparison of the respective spectral functions involves a correction from isospin-breaking effects, which is evaluated. After the correction it is found that the dominant $\pi\pi$ spectral functions do not agree within experimental and theoretical uncertainties. Some disagreement is also found for the 4π spectral functions. The consequences of these discrepancies for vacuum polarization calculations are presented, with the emphasis on the muon anomalous magnetic moment. Adding quadratically experimental and theoretical uncertainties, we find that the full Standard Model prediction of a_μ deviates from the recent BNL measurement at the level of 3.0 (e^+e^- -based) and 0.9 (τ -based) standard deviations.

1. INTRODUCTION

Hadronic vacuum polarization in the photon propagator plays an important role in the precision tests of the Standard Model. This is the case for the evaluation of the electromagnetic coupling at the Z mass scale, $\alpha(M_Z^2)$, which receives a contribution $\Delta\alpha_{\text{had}}(M_Z^2)$ of the order of $2.8 \cdot 10^{-2}$ that must be known to an accuracy of better than 1% so that it does not limit the accuracy on the indirect determination of the Higgs boson mass from the measurement of $\sin^2\theta_W$. Another example is provided by the anomalous magnetic moment $a_\mu = (g_\mu - 2)/2$ of the muon, where the hadronic vacuum polarization component is the leading contributor to the uncertainty of the theoretical prediction.

Starting from Refs. [1,2] there is a long history of calculating the contributions from hadronic vacuum polarization in these processes. As they cannot be obtained from first principles because of the low energy scale involved, the computation relies on analyticity and unitarity so that the rele-

vant integrals can be expressed in terms of an experimentally determined spectral function which is proportional to the cross section for e^+e^- annihilation into hadrons. The accuracy of the calculations has therefore followed the progress in the quality of the corresponding data [3]. Because the latter was not always suitable, it was deemed necessary to resort to other sources of information. One such possibility was the use [4] of the vector spectral functions derived from the study of hadronic τ decays [5] for the energy range less than 1.8 GeV. Another one occurred when it was realized in the study of τ decays [6] that perturbative QCD could be applied to energy scales as low as 1-2 GeV, thus offering a way to replace poor e^+e^- data in some energy regions by a reliable and precise theoretical prescription [7-9]. Finally, without any further theoretical assumption, it was proposed to use QCD sum rules [10,11] in order to improve the evaluation in energy regions dominated by resonances where one has to rely on experimental data. Using these improvements the lowest-order hadronic contribution to a_μ was

*Work done in collaboration with M. Davier, S. Eidelman and Z. Zhang

found to be [11]

$$a_{\mu}^{\text{had,LO}} = (692.4 \pm 6.2) \cdot 10^{-10} . \quad (1)$$

The complete theoretical prediction includes in addition QED, weak and higher order hadronic contributions.

The anomalous magnetic moment of the muon is experimentally known to very high accuracy. Combined with the older, less precise results from CERN [12], the measurements from the E821 experiment at BNL [13–15], including the most recent result [16], yield

$$a_{\mu}^{\text{exp}} = (11\,659\,203 \pm 8) \cdot 10^{-10} , \quad (2)$$

and are aiming at an ultimate precision of $4 \cdot 10^{-10}$ in the future. The previous experimental result [15] was found to deviate from the theoretical prediction by 2.6σ , but a large part of the discrepancy was originating from a sign mistake in the calculation of the small contribution from the so-called light-by-light (LBL) scattering diagrams [17,18]. The new calculations of the LBL contribution [19–21] have reduced the discrepancy to a nonsignificant 1.6σ level. At any rate it is clear that the presently achieved experimental accuracy already calls for a more precise evaluation of $a_{\mu}^{\text{had,LO}}$.

New experimental and theoretical developments have prompted the re-evaluation of the hadronic contributions presented in Ref. [22] and reported here:

- new, precise results have been obtained at Novosibirsk with the CMD-2 detector in the region dominated by the ρ resonance [23], and more accurate R measurements have been performed in Beijing with the BES detector in the 2-5 GeV energy range [24].
- new preliminary results are available from the final analysis of τ decays with ALEPH using the full statistics accumulated at LEP1 [25]; also the information from the spectral functions measured by CLEO [26, 27] and OPAL [28] has been incorporated in the analysis.
- new results on the evaluation of isospin breaking have been produced [29–31], thus

providing a better understanding of this critical area when relating vector τ and isovector e^+e^- spectral functions.

2. MUON MAGNETIC ANOMALY

It is convenient to separate the Standard Model prediction for the anomalous magnetic moment of the muon into its different contributions,

$$a_{\mu}^{\text{SM}} = a_{\mu}^{\text{QED}} + a_{\mu}^{\text{had}} + a_{\mu}^{\text{weak}} , \quad (3)$$

with $a_{\mu}^{\text{had}} = a_{\mu}^{\text{had,LO}} + a_{\mu}^{\text{had,HO}} + a_{\mu}^{\text{had,LBL}}$, where $a_{\mu}^{\text{QED}} = (11\,658\,470.6 \pm 0.3) \cdot 10^{-10}$ is the pure electromagnetic contribution (see [32,33] and references therein), $a_{\mu}^{\text{had,LO}}$ is the lowest-order contribution from hadronic vacuum polarization, $a_{\mu}^{\text{had,HO}} = (-10.0 \pm 0.6) \cdot 10^{-10}$ is the corresponding higher-order part [34,4], and $a_{\mu}^{\text{weak}} = (15.4 \pm 0.1 \pm 0.2) \cdot 10^{-10}$, where the first error is the hadronic uncertainty and the second is due to the Higgs mass range, accounts for corrections due to exchange of the weakly interacting bosons up to two loops [35]. For the LBL part we add the values for the pion-pole contribution [19–21] and the other terms [20,21] to obtain $a_{\mu}^{\text{had,LBL}} = (8.6 \pm 3.5) \cdot 10^{-10}$.

By virtue of the analyticity of the vacuum polarization correlator, the contribution of the hadronic vacuum polarization to a_{μ} can be calculated via the dispersion integral [36]

$$a_{\mu}^{\text{had,LO}} = \frac{\alpha^2(0)}{3\pi^2} \int_{4m_{\pi}^2}^{\infty} ds \frac{K(s)}{s} R(s) , \quad (4)$$

where $K(s)$ is the QED kernel [37] strongly emphasizing the low-energy spectral functions in the integral (4). In effect, about 91% of the total contribution to $a_{\mu}^{\text{had,LO}}$ is accumulated at center-of-mass energies \sqrt{s} below 1.8 GeV and 73% of $a_{\mu}^{\text{had,LO}}$ is covered by the two-pion final state which is dominated by the $\rho(770)$ resonance. In Eq. (4), $R(s) \equiv R^{(0)}(s)$ denotes the ratio of the 'bare' cross section for e^+e^- annihilation into hadrons to the pointlike muon-pair cross section. At low mass-squared, $R(s)$ is taken from experiment.

3. DATA FROM e^+e^- ANNIHILATION

The exclusive low energy e^+e^- cross sections have been measured mainly by experiments running at e^+e^- colliders in Novosibirsk and Orsay. Due to the high hadron multiplicity at energies above ~ 2.5 GeV, the exclusive measurement of the respective hadronic final states is not practicable. Consequently, the experiments at the high energy colliders have measured the total inclusive cross section ratio R .

The most precise data from CMD-2 on the $e^+e^- \rightarrow \pi^+\pi^-$ cross sections are now available in their final form [23]. They differ from the preliminary ones, released two years ago [38], mostly in the treatment of the radiative corrections. The various changes resulted in a reduction of the cross section by about 1% below the ρ peak and 5% above. The overall systematic error of the final data is quoted to be 0.6% and is dominated by the uncertainties in the radiative corrections (0.4%). Agreement is observed between CMD-2 and the previous experiments within the much larger uncertainties (2-10%) quoted by the latter.

Large discrepancies are observed between the different data sets for the $e^+e^- \rightarrow \pi^+\pi^-\pi^0\pi^0$ cross sections (see Fig. 5). These are probably related to problems in the calculation of the detection efficiency, since the efficiencies are small in general ($\sim 10 - 30\%$) and they are affected by uncertainties in the decay dynamics that is assumed in the Monte Carlo simulation. One could expect the more recent experiments (CMD-2 [40] and SND [41]) to be more reliable in this context because of specific studies performed in order to identify the major decay processes involved.

For $e^+e^- \rightarrow \pi^+\pi^-\pi^+\pi^-$ the experiments agree reasonably well within their quoted uncertainties (see Fig. 4 in Section 7).

A detailed compilation and complete references of all the data used for this analysis are given in Ref. [22].

4. DATA FROM HADRONIC τ DECAYS

Data from τ decays into two- and four-pion final states $\tau^- \rightarrow \nu_\tau \pi^-\pi^0$, $\tau^- \rightarrow \nu_\tau \pi^- 3\pi^0$ and $\tau^- \rightarrow \nu_\tau 2\pi^-\pi^+\pi^0$, are available from

ALEPH [25,5], CLEO [26,27] and OPAL [28]. The branching fraction $B_{\pi\pi^0}$ for the $\tau \rightarrow \nu_\tau \pi^-\pi^0$ (γ) decay mode is of particular interest since it provides the normalization of the corresponding spectral function. The new value [25], $B_{\pi\pi^0} = (25.47 \pm 0.13) \%$, turns out to be larger than the previously published one [42] based on the 1991-93 LEP1 statistics, $(25.30 \pm 0.20) \%$.

In the limit of isospin invariance, the corresponding e^+e^- isovector cross sections are calculated via the isospin rotations

$$\sigma_{e^+e^- \rightarrow \pi^+\pi^-}^{I=1} = \frac{4\pi\alpha^2}{s} v_{\pi^-\pi^0}, \quad (5)$$

$$\sigma_{e^+e^- \rightarrow \pi^+\pi^-\pi^+\pi^-}^{I=1} = 2 \cdot \frac{4\pi\alpha^2}{s} v_{\pi^- 3\pi^0}, \quad (6)$$

$$\sigma_{e^+e^- \rightarrow \pi^+\pi^-\pi^0\pi^0}^{I=1} = \frac{4\pi\alpha^2}{s} \left[v_{2\pi^-\pi^+\pi^0} - v_{\pi^- 3\pi^0} \right]. \quad (7)$$

The τ spectral function $v_V(s)$ for a given vector hadronic state V is defined by [43]

$$v_V(s) \propto \frac{B(\tau^- \rightarrow \nu_\tau V^-)}{B(\tau^- \rightarrow \nu_\tau e^- \bar{\nu}_e)} \frac{dN_V}{N_V ds} \times \left[\left(1 - \frac{s}{m_\tau^2}\right)^2 \left(1 + \frac{2s}{m_\tau^2}\right) \right]^{-1}, \quad (9)$$

where $|V_{ud}| = 0.9748 \pm 0.0010$ (using [44]). The spectral functions are obtained from the corresponding invariant mass distributions, after subtracting out the non- τ background and the feedthrough from other τ decay channels, and after a final unfolding from detector effects such as energy and angular resolutions, acceptance, calibration and photon identification. Agreement within errors is observed for the three input spectral functions $v_{\pi^-\pi^0}$ (ALEPH, CLEO, OPAL), so that we use their weighted average in the following.

5. RADIATIVE CORRECTIONS FOR e^+e^- DATA

Radiative corrections applied to the measured e^+e^- cross sections are an important step in the

experimental analyses. They involve the consideration of several physical processes and lead to large corrections. We stress that the evaluation of the integral in Eq. (4) requires the use of the 'bare' hadronic cross section, so that the input data must be analyzed with care in this respect. Several steps are to be considered:

- Corrections are applied to the luminosity determination, based on large-angle Bhabha scattering and muon-pair production in the low-energy experiments, and small-angle Bhabha scattering at high energies. These processes are usually corrected for external radiation, vertex corrections and vacuum polarization from lepton loops.
- The hadronic cross sections given by the experiments are in general corrected for initial state radiation and the effect of loops at the electron vertex.
- The vacuum polarization correction in the photon propagator is a more delicate point. The cross sections need to be fully corrected for our use, *i.e.* $\sigma_{\text{bare}} = \sigma_{\text{dressed}}(\alpha(0)/\alpha(s))^2$, where σ_{dressed} is the measured cross section already corrected for initial state radiation, and $\alpha(s)$ is obtained from resummation of the lowest-order evaluation, giving $\alpha(s) = \alpha(0)/(1 - \Delta\alpha_{\text{lep}}(s) - \Delta\alpha_{\text{had}}(s))$. Whereas $\Delta\alpha_{\text{lep}}(s)$ can be calculated analytically, $\Delta\alpha_{\text{had}}(s)$ is related by analyticity and unitarity to a dispersion integral, akin to Eq. (4). Since the hadronic correction involves the knowledge of $R(s)$ at all energies, including those where the measurements are made, the procedure has to be iterative, and requires experimental as well as theoretical information over a large energy range.

The new data from CMD-2 [23] are explicitly corrected for both leptonic and hadronic vacuum polarization effects, whereas the preliminary data from the same experiment [38] and data from other experiments were not (see follow up of this discussion in Ref. [22])

Table 1

Expected sources of isospin symmetry breaking between e^+e^- and τ spectral functions in the 2π and 4π channels, and the corresponding corrections to $a_\mu^{\text{had,LO}}$ as obtained from τ data.

Sources of Isospin Symmetry Breaking	$\Delta a_\mu^{\text{had,LO}} (10^{-10})$ $\pi^+\pi^-$
Short distance rad. corr.	-12.1 ± 0.3
Long distance rad. corr.	-1.0
$m_{\pi^-} \neq m_{\pi^0}$ (β in cross section)	-7.0
$m_{\pi^-} \neq m_{\pi^0}$ (β in ρ width)	$+4.2$
$m_{\rho^-} \neq m_{\rho^0}$	0 ± 2.0
$\rho - \omega$ interference	$+3.5 \pm 0.6$
Electromagnetic decay modes	-1.4 ± 1.2
Sum	-13.8 ± 2.4

- In Eq. (4) one must incorporate in $R(s)$ the contributions of all hadronic states produced at the energy \sqrt{s} . In particular, radiative effects in the hadronic final state must be considered, *i.e.*, final states such as $V + \gamma$ (FSR) have to be included. While FSR has been added to the newest CMD-2 data [23], this is not the case for the older data and thus has to be corrected for [22] "by hand", using an analytical expression computed in scalar QED (point-like pions) [45].

In summary, we correct each e^+e^- experimental result, but those from CMD-2 ($\pi\pi$), by the factor $C_{\text{HVP}} \cdot C_{\text{FSR}}$, where C_{HVP} accounts for hadronic vacuum polarization and C_{FSR} stands for the FSR correction. We assign uncertainties of 50% (vacuum polarization) and 100% (FSR corrections), which are considered to be fully correlated between all channels to which the corrections apply.

6. ISOSPIN BREAKING IN e^+e^- AND τ SPECTRAL FUNCTIONS

The relationships (5), (6) and (7) between e^+e^- and τ spectral functions only hold in the limit of exact isospin invariance. This is the Conserved

Vector Current (CVC) property of weak decays. It follows from the factorization of strong interaction physics as produced through the γ and W propagators out of the QCD vacuum. However, we know that we must expect symmetry breaking at some level from electromagnetic effects and even in QCD because of the up and down quark mass splitting. Since the normalization of the τ spectral functions is experimentally known at the 0.5% level, it is clear that isospin-breaking effects must be carefully examined if one wants this precision to be maintained in the vacuum polarization integrals.

Because of the dominance of the $\pi\pi$ contribution in the energy range of interest for τ data, we discuss mainly this channel, following our earlier analysis [4]. The corrections on $a_\mu^{\text{had,LO}}$ from isospin breaking are given in Table 1. A more complete discussion, in particular with respect to the corrections previously applied is given in Ref. [22].

The dominant contribution to the electroweak radiative corrections stems from the short distance correction to the effective four-fermion coupling $\tau^- \rightarrow \nu_\tau (d\bar{u})^-$ enhancing the τ amplitude by the factor $S_{\text{EW}}^{\text{had}} = 1.0194$ [46]. This correction leaves out the possibility of sizeable contributions from virtual loops. This problem was studied in Ref. [30] within a model based on Chiral Perturbation Theory. In this way the correct low-energy hadronic structure is implemented and a consistent framework has been set up to calculate electroweak and strong processes, such as the radiative corrections in the $\tau \rightarrow \nu_\tau \pi^- \pi^0$ decay. Their new analysis [31] directly applies to the inclusive radiative rate, $\tau \rightarrow \nu_\tau \pi^- \pi^0 (\gamma)$, as measured by the experiments. The relation between the Born level e^+e^- spectral function and the τ spectral function reads [31]

$$v_{\pi^+\pi^-} = \frac{1}{G_{\text{EM}}} \frac{\beta_0^3}{\beta_-^3} \left| \frac{F_\pi^0}{F_\pi^-} \right|^2 v_{\pi^-\pi^0(\gamma)}, \quad (10)$$

where $G_{\text{EM}} \equiv G_{\text{EM}}(s)$ is the long-distance radiative correction involving both real photon emission and virtual loops (the infrared divergence cancels in the sum). Note that the short-distance S_{EW} correction, discussed above, is already applied in the definition of v_- (*cf.* Eq. (9)), but

its value differs from the one given in Ref. [46], because subleading quark-level and hadron-level contributions should not be added, as double counting would occur. The correct expression for the $\pi^-\pi^0$ mode therefore reads

$$\frac{S_{\text{EW}}^{\text{had}} G_{\text{EM}}}{S_{\text{EW}}^{\text{sub,lep}}} = (1.0233 \pm 0.0006) \cdot G_{\text{EM}}, \quad (11)$$

the subleading hadronic corrections being now incorporated in the mass-squared-dependent G_{EM} factor. Equation (10) explicitly corrects for the mass difference between neutral and charged pions affecting the cross section and the width of the ρ .

The different contributions to the isospin-breaking corrections are shown in the second column of Table 1. The dominant uncertainty stems from the ρ^\pm - ρ^0 mass difference.

Since the integral (4) requires as input the e^+e^- spectral function including FSR photon emission, a final correction is necessary. It is identical to that applied in the CMD-2 analysis [23,45] (*cf.* Section 5). The total correction to the τ result amounts to $(-9.3 \pm 2.4) 10^{-10}$.

There exists no comparable study of isospin breaking in the 4π channels. Only kinematic corrections resulting from the pion mass difference have been considered so far [29], which we have applied in this analysis. It creates shifts of $-0.7 10^{-10}$ (-3.8%) and $+0.1 10^{-10}$ ($+1.1\%$) for $2\pi^+2\pi^-$ and $\pi^+\pi^-2\pi^0$, respectively.

7. COMPARISON OF e^+e^- AND τ SPECTRAL FUNCTIONS

The e^+e^- and the isospin-breaking corrected τ spectral functions can be directly compared for the dominant 2π and 4π final states. For the 2π channel, the ρ -dominated form factor falls off very rapidly at high energy so that the comparison can be performed in practice over the full energy range of interest. The situation is different for the 4π channels where the τ decay kinematics limits the exercise to energies less than ~ 1.6 GeV, with only limited statistics beyond.

Fig. 3 shows the comparison for the 2π spectral functions. Visually, the agreement seems satisfactory, however the large dynamical range involved

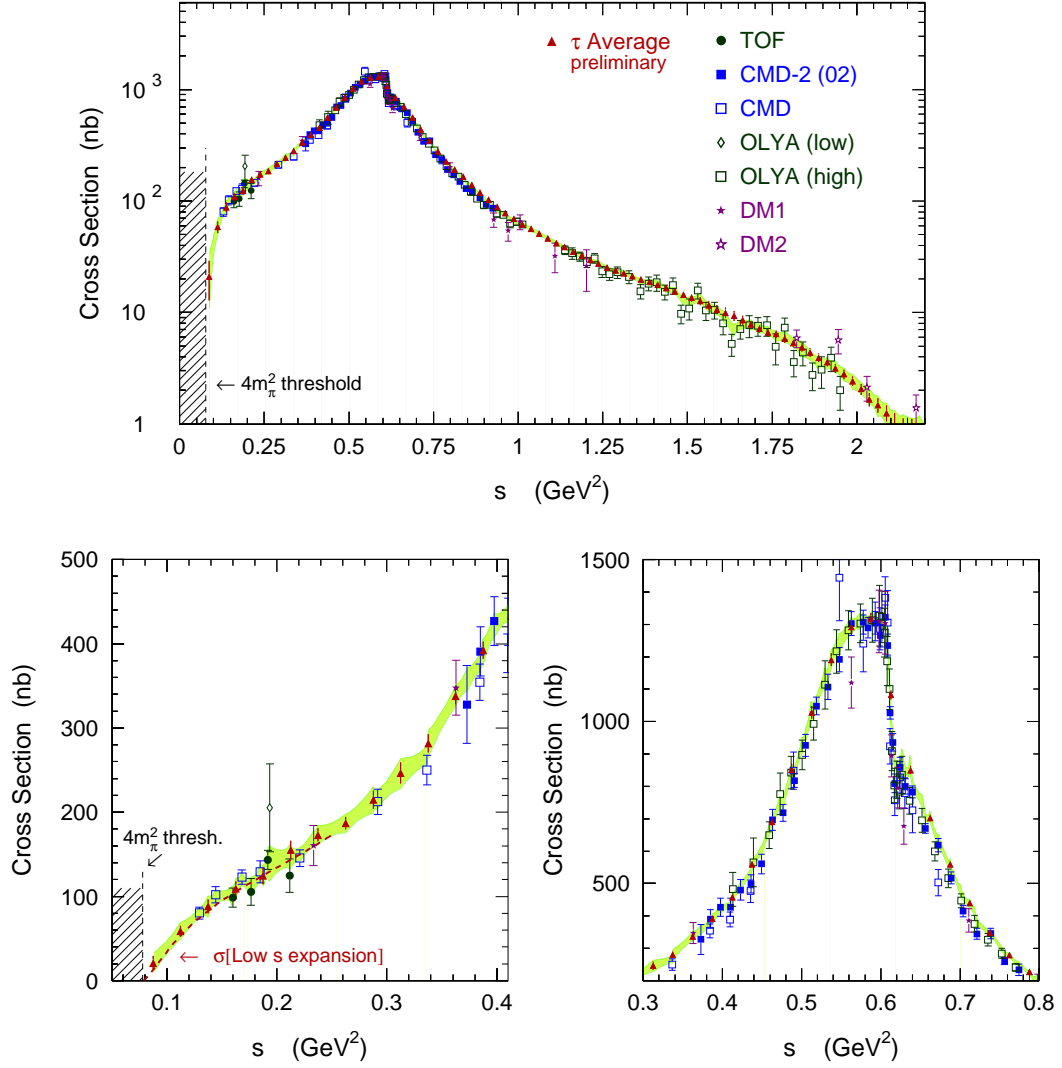


Figure 3. Comparison of the $\pi^+\pi^-$ spectral functions from e^+e^- and isospin-breaking corrected τ data, expressed as e^+e^- cross sections. The band indicates the combined e^+e^- and τ result within 1σ errors. It is given for illustration purpose only.

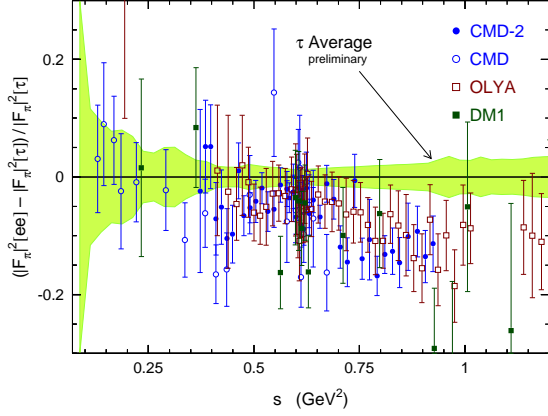


Figure 1. Relative comparison of the $\pi^+\pi^-$ spectral functions from e^+e^- and isospin-breaking corrected τ data, expressed as a ratio to the τ spectral function. The band shows the uncertainty on the latter.

does not permit an accurate test. To do so, the e^+e^- data are plotted as a point-by-point ratio to the τ spectral function in Fig. 1, and enlarged in Fig. 2, to better emphasize the region of the ρ peak. The e^+e^- data are significantly lower by 2-3% below the peak, the discrepancy increasing to about 10% in the 0.9-1.0 GeV region.

The comparison for the 4π cross sections is given in Fig. 4 for the $2\pi^+2\pi^-$ channel and in Fig. 5 for $\pi^+\pi^-2\pi^0$. The latter suffers from large differences between the results from the different e^+e^- experiments. The τ data, combining two measured spectral functions according to Eq. (7) and corrected for isospin breaking as discussed in Section 6, lie somewhat in between with large uncertainties above 1.4 GeV because of the lack of statistics and a large feedthrough background in the $\tau \rightarrow \nu_\tau \pi^- 3\pi^0$ mode. In spite of these difficulties the $\pi^- 3\pi^0$ spectral function is in agreement with e^+e^- data as can be seen in Fig. 4. It is clear that intrinsic discrepancies exist among the e^+e^- experiments and that a quantitative test of CVC in the $\pi^+\pi^-2\pi^0$ channel is premature.

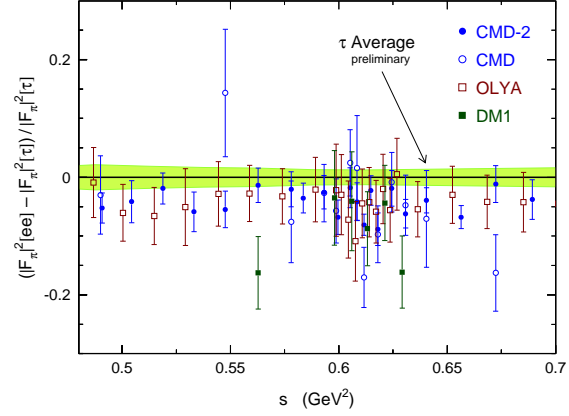


Figure 2. Relative comparison in the ρ region of the $\pi^+\pi^-$ spectral functions from e^+e^- and isospin-breaking corrected τ data, expressed as a ratio to the τ spectral function. The band shows the uncertainty on the latter.

7.1. Branching Ratios in τ Decays and CVC

A convenient way to assess the compatibility between e^+e^- and τ spectral functions proceeds with the evaluation of τ decay fractions using the relevant e^+e^- spectral functions as input. All the isospin-breaking corrections discussed in Section 6 are included. The advantage of this procedure is to allow a quantitative comparison using a single number. The weighting of the spectral function is however different from the vacuum polarization kernels. Using the branching fraction $B(\tau^- \rightarrow \nu_\tau e^- \bar{\nu}_e) = (17.810 \pm 0.039)\%$, obtained assuming leptonic universality in the charged weak current [25], the results for the main channels are given in Table 2. The errors quoted for the CVC values are split into uncertainties from (i) the experimental input (the e^+e^- annihilation cross sections) and the numerical integration procedure, (ii) the missing radiative corrections applied to the relevant e^+e^- data, and (iii) the isospin-breaking corrections when relating τ and e^+e^- spectral functions. The values for the τ branching ratios involve measurements [25,47,48] given without charged hadron identification, *i.e.*, for

Table 2

Branching fractions of τ vector decays into 2 and 4 pions in the final state. Second column: world average. Third column: inferred from e^+e^- spectral functions using the isospin relations (5-7) and correcting for isospin breaking. The experimental error of the $\pi^+\pi^-$ CVC value contains an absolute procedural integration error of 0.08%. Experimental errors, including uncertainties on the integration procedure, and theoretical (missing radiative corrections for e^+e^- , and isospin-breaking corrections and V_{ud} for τ) are shown separately. Right column: differences between the direct measurements in τ decays and the CVC evaluations, where the separate errors have been added in quadrature.

Mode	τ data	Branching fractions (in %) e^+e^- via CVC	$\Delta(\tau - e^+e^-)$
$\tau^- \rightarrow \nu_\tau \pi^- \pi^0$	25.46 ± 0.12	$23.98 \pm \underbrace{0.25_{\text{exp}} \pm 0.11_{\text{rad}} \pm 0.12_{\text{SU}(2)}}_{0.30}$	$+1.48 \pm 0.32$
$\tau^- \rightarrow \nu_\tau \pi^- 3\pi^0$	1.01 ± 0.08	$1.09 \pm \underbrace{0.06_{\text{exp}} \pm 0.02_{\text{rad}} \pm 0.05_{\text{SU}(2)}}_{0.08}$	-0.08 ± 0.11
$\tau^- \rightarrow \nu_\tau 2\pi^- \pi^+ \pi^0$	4.54 ± 0.13	$3.63 \pm \underbrace{0.19_{\text{exp}} \pm 0.04_{\text{rad}} \pm 0.09_{\text{SU}(2)}}_{0.21}$	$+0.91 \pm 0.25$

the $h\pi^0\nu_\tau$, $h3\pi^0\nu_\tau$ and $3h\pi^0\nu_\tau$ final states. The corresponding channels with charged kaons have been measured [49,50] and their contributions can be subtracted out in order to obtain the pure pionic modes. As expected from the preceding discussion, a large discrepancy is observed for the $\tau \rightarrow \nu_\tau \pi^- \pi^0$ branching ratio, with a difference of $(-1.48 \pm 0.12_\tau \pm 0.25_{\text{ee}} \pm 0.11_{\text{rad}} \pm 0.12_{\text{SU}(2)})\%$, where the uncertainties are from the τ branching ratio, e^+e^- cross sections, e^+e^- missing radiative corrections and isospin-breaking corrections (including the uncertainty on V_{ud}), respectively. Adding all errors in quadrature, the effect represents a 4.6σ discrepancy. Since the disagreement between e^+e^- and τ spectral functions is more pronounced at energies above 750 MeV, we expect a smaller discrepancy in the calculation of $a_\mu^{\text{had,LO}}$ because of the steeply falling kernel $K(s)$ in this case.

The situation in the 4π channels is different. Agreement is observed for the $\pi^- 3\pi^0$ mode within an accuracy of 11%, however the comparison is not satisfactory for the $2\pi^- \pi^+ \pi^0$ mode. In the latter case, the relative difference is very large, $(22 \pm 6)\%$, compared to any reasonable level of isospin symmetry breaking. As such, it rather points to experimental problems that have to be

investigated.

8. SPECIFIC CONTRIBUTIONS

In some energy regions where data information is scarce and reliable theoretical predictions are available, we use analytical contributions to extend the experimental integral. Also, the treatment of narrow resonances involves a specific procedure.

8.1. The $\pi^+\pi^-$ Threshold Region

To overcome the lack of precise data at threshold energies and to benefit from the analyticity property of the pion form factor, a third order expansion in s is used. The pion form factor F_π^0 is connected with the $\pi^+\pi^-$ cross section via $|F_\pi^0|^2 = (3s/\pi\alpha^2\beta_0^3)\sigma_{\pi\pi}$. The expansion for small s reads

$$F_\pi^0 = 1 + \frac{1}{6}\langle r^2 \rangle_\pi s + c_1 s^2 + c_2 s^3 + O(s^4), \quad (12)$$

where we use $\langle r^2 \rangle_\pi = (0.439 \pm 0.008) \text{ fm}^2$ [51], and the two parameters $c_{1,2}$ are fitted to the data in the range $[2m_\pi, 0.6 \text{ GeV}]$. The results of the fits are explicitly quoted in Ref. [22]. We show the functions obtained in Fig. 6. Good agreement is observed in the low energy region where

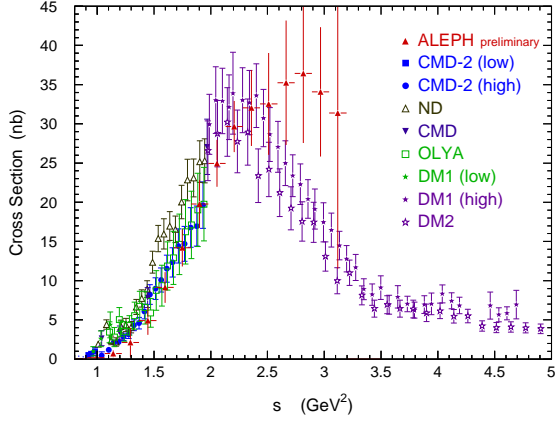


Figure 4. Comparison of the $2\pi^+2\pi^-$ spectral functions from e^+e^- and isospin-breaking corrected τ data, expressed as e^+e^- cross sections.

the expansion should be reliable. Since the fits incorporate unquestionable constraints from first principles, we have chosen to use this parameterization for evaluating the integrals in the range up to 0.5 GeV.

8.2. Integration over the ω and ϕ Resonances

In the regions around the ω and ϕ resonances we have assumed in the preceding works that the cross section of the $\pi^+\pi^-\pi^0$ production on the one hand, and the $\pi^+\pi^-\pi^0$, K^+K^- as well as $K_S^0K_L^0$ production on the other hand is saturated by the corresponding resonance production. In a data driven approach it is however more careful to directly integrate the measurement points without introducing prior assumptions on the underlying process dynamics [52]. Possible non-resonant contributions and interference effects are thus accounted for.

Notwithstanding, a straightforward trapezoidal integration buries the danger of a bias: with insufficient scan density, the linear interpolation of the measurements leads to a significant overesti-

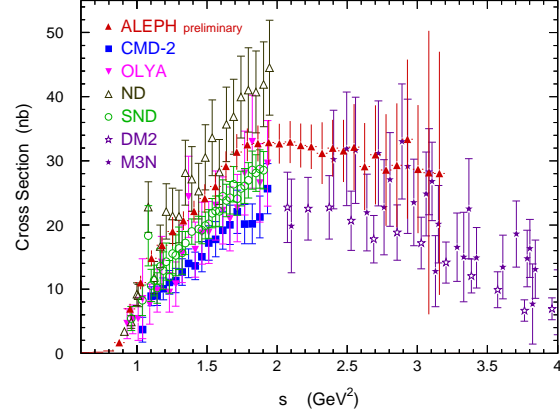


Figure 5. Comparison of the $\pi^+\pi^-2\pi^0$ spectral functions from e^+e^- and isospin-breaking corrected τ data, expressed as e^+e^- cross sections.

mation of the integral when dealing with strongly concave functions such as the tails of Breit-Wigner resonance curves.

We therefore perform a phenomenological fit of a BW resonance plus two Gaussians (only one Gaussian is necessary for the ω) to account for contributions other than the single resonance. Both fits result in satisfactory χ^2 values. We have accounted for the systematics due to the arbitrariness in the choice of the parametrization by varying the functions and parameters used. The resulting effects are numerically small compared to the experimental errors.

Since the experiments quote the cross section results without correcting for leptonic and hadronic vacuum polarization in the photon propagator, we perform the correction here. The correction of hadronic vacuum polarization being iterative and thus only approximative, we assign half of the total vacuum polarization correction as generous systematic errors (*cf.* Section 5). In spite of that, the evaluation of $a_\mu^{\text{had,LO}}$ is dominated by the experimental uncertainties. Since the trapezoidal rule is biased, we choose the re-

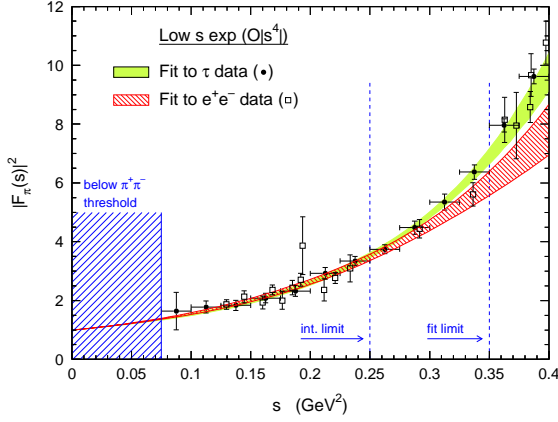


Figure 6. Fit of the pion form factor from $4m_\pi^2$ to 0.35 GeV^2 using a third-order Taylor expansion with the constraints at $s = 0$ and the measured pion r.m.s. charge radius from space-like data [51]. The result of the fit is integrated only up to 0.25 GeV^2 .

sults based on the BW fits for the final evaluation of $a_\mu^{\text{had,LO}}$.

8.3. Narrow $c\bar{c}$ and $b\bar{b}$ Resonances

The contributions from the narrow J/ψ resonances are computed using a relativistic Breit-Wigner parametrization for their line shape. The physical values for the resonance parameters and their errors are taken from the latest compilation in Ref. [44]. Vacuum polarization effects are already included in the quoted leptonic widths. The total parametrization errors are then calculated by Gaussian error propagation. This integration procedure is not followed for the $\psi(3S)$ state which is already included in the R measurements, and for the Υ resonances which are represented in an average sense (global quark-hadron duality) by the $b\bar{b}$ QCD contribution, discussed next.

8.4. QCD Prediction at High Energy

Since the emphasis in this paper is on a complete and critical evaluation of spectral functions from low-energy data, we have adopted the conservative choice of using the QCD prediction only above an energy of 5 GeV . The details of the

calculation can be found in our earlier publications [7,11,22] and in the references therein.

A test of the QCD prediction can be performed in the energy range between 1.8 and 3.7 GeV . The contribution to $a_\mu^{\text{had,LO}}$ in this region is computed to be $(33.87 \pm 0.46) \cdot 10^{-10}$ using QCD, to be compared with the result, $(34.9 \pm 1.8) \cdot 10^{-10}$ from the data. The two values agree within the 5% accuracy of the measurements.

9. RESULTS

9.1. Lowest Order Hadronic Contributions

We use the trapezoidal rule to integrate the experimental data points (with the exception of the narrow resonances). Correlations between the measurements as well as among experiments have been taken into account [22]. Before adding up all the contributions to $a_\mu^{\text{had,LO}}$, we shall summarize the procedure. On the one hand, the e^+e^- -based evaluation is done in three pieces: the sum of exclusive channels below 2 GeV , the R measurements in the 2 - 5 GeV range and the QCD prediction for R above. Major contributions stem from the 2π (73%) and the two 4π (4.5%) channels. On the other hand, in the τ -based evaluation, the latter three contributions are taken from τ data up to 1.6 GeV and complemented by e^+e^- data above, because the τ spectral functions run out of precision near the kinematic limit of the τ mass. Thus, for nearly 77% of $a_\mu^{\text{had,LO}}$ (contributing 80% of the total error-squared), two independent evaluations (e^+e^- and τ) are produced, the remainder being computed from e^+e^- data and QCD alone.

Fig. 7 gives a panoramic view of the e^+e^- data in the relevant energy range. The shaded band below 2 GeV represents the sum of the exclusive channels considered in the analysis. It turns out to be smaller than our previous estimate [4], essentially because more complete data sets are used and new information on the dynamics could be incorporated in the isospin constraints for the missing channels. The QCD prediction is indicated by the cross-hatched band. It is used in this analysis only for energies above 5 GeV . Note that the QCD band is plotted taking into account the thresholds for open flavour B states, in order

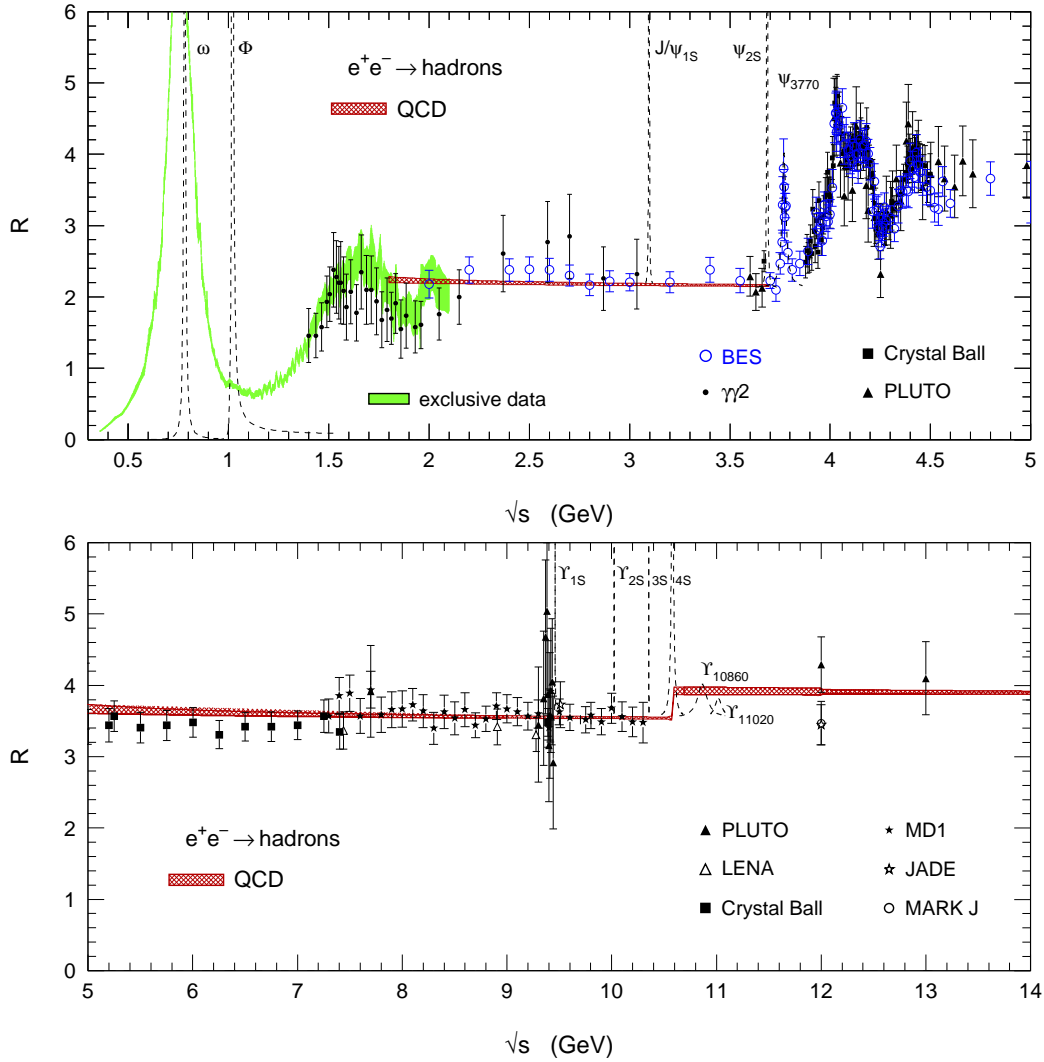


Figure 7. Compilation of the data contributing to $a_\mu^{\text{had,LO}}$. Shown is the total hadronic over muonic cross section ratio R . The shaded band below 2 GeV represents the sum of the exclusive channels considered in this analysis, with the exception of the contributions from the narrow resonances which are given as dashed lines. All data points shown correspond to inclusive measurements. The cross-hatched band gives the prediction from (essentially) perturbative QCD, which is found to be in good agreement with the measurements in the continuum above 2 GeV. In this figure the $b\bar{b}$ threshold is indicated at the onset of $B\bar{B}$ states in order to facilitate the comparison with data in the continuum. In the actual calculation the threshold is taken at twice the pole mass of the b quark.

Table 3

Summary of the $a_\mu^{\text{had,LO}}$ contributions from e^+e^- annihilation and τ decays. The uncertainties on the vacuum polarization and FSR corrections are given as second errors in the individual e^+e^- contributions, while those from isospin breaking are similarly given for the τ contributions. These 'theoretical' uncertainties are correlated among all channels, except in the case of isospin breaking which shows little correlation between the 2π and 4π channels. The errors given for the sums in the last line are from the experiment, the missing radiative corrections in e^+e^- and, in addition for τ , SU(2) breaking.

Modes	Energy [GeV]	e^+e^-	$a_\mu^{\text{had,LO}} (10^{-10})$ $\tau^{(3)}$	$\Delta(e^+e^- - \tau)$
Low s exp. $\pi^+\pi^-$	$[2m_{\pi^\pm} - 0.500]$	$58.04 \pm 1.70 \pm 1.14$	$56.03 \pm 1.61 \pm 0.28$	$+2.0 \pm 2.6$
$\pi^+\pi^-$	$[0.500 - 1.800]$	$440.81 \pm 4.65 \pm 1.54$	$464.03 \pm 3.19 \pm 2.34$	-23.2 ± 6.3
$\pi^0\gamma, \eta\gamma^{(1)}$	$[0.500 - 1.800]$	$0.93 \pm 0.15 \pm 0.01$	-	-
ω	$[0.300 - 0.810]$	$36.94 \pm 0.84 \pm 0.80$	-	-
$\pi^+\pi^-\pi^0$ [below ϕ]	$[0.810 - 1.000]$	$4.20 \pm 0.40 \pm 0.05$	-	-
ϕ	$[1.000 - 1.055]$	$34.80 \pm 0.92 \pm 0.64$	-	-
$\pi^+\pi^-\pi^0$ [above ϕ]	$[1.055 - 1.800]$	$2.45 \pm 0.26 \pm 0.03$	-	-
$\pi^+\pi^-2\pi^0$	$[1.020 - 1.800]$	$16.73 \pm 1.32 \pm 0.20$	$21.44 \pm 1.33 \pm 0.60$	-4.7 ± 1.8
$2\pi^+2\pi^-$	$[0.800 - 1.800]$	$13.95 \pm 0.90 \pm 0.23$	$12.34 \pm 0.96 \pm 0.40$	$+1.6 \pm 2.0$
$2\pi^+2\pi^-\pi^0$	$[1.019 - 1.800]$	$2.09 \pm 0.43 \pm 0.04$	-	-
$\pi^+\pi^-3\pi^0^{(2)}$	$[1.019 - 1.800]$	$1.29 \pm 0.22 \pm 0.02$	-	-
$3\pi^+3\pi^-$	$[1.350 - 1.800]$	$0.10 \pm 0.10 \pm 0.00$	-	-
$2\pi^+2\pi^-2\pi^0$	$[1.350 - 1.800]$	$1.41 \pm 0.30 \pm 0.03$	-	-
$\pi^+\pi^-4\pi^0^{(2)}$	$[1.350 - 1.800]$	$0.06 \pm 0.06 \pm 0.00$	-	-
$\eta(\rightarrow \pi^+\pi^-\gamma, 2\gamma)\pi^+\pi^-$	$[1.075 - 1.800]$	$0.54 \pm 0.07 \pm 0.01$	-	-
$\omega(\rightarrow \pi^0\gamma)\pi^0$	$[0.975 - 1.800]$	$0.63 \pm 0.10 \pm 0.01$	-	-
$\omega(\rightarrow \pi^0\gamma)(\pi\pi)^0$	$[1.340 - 1.800]$	$0.08 \pm 0.01 \pm 0.00$	-	-
K^+K^-	$[1.055 - 1.800]$	$4.63 \pm 0.40 \pm 0.06$	-	-
$K_S^0 K_L^0$	$[1.097 - 1.800]$	$0.94 \pm 0.10 \pm 0.01$	-	-
$K^0 K^\pm \pi^\mp^{(2)}$	$[1.340 - 1.800]$	$1.84 \pm 0.24 \pm 0.02$	-	-
$K\bar{K}\pi^0^{(2)}$	$[1.440 - 1.800]$	$0.60 \pm 0.20 \pm 0.01$	-	-
$K\bar{K}\pi\pi^{(2)}$	$[1.441 - 1.800]$	$2.22 \pm 1.02 \pm 0.03$	-	-
$R = \sum \text{excl. modes}$	$[1.800 - 2.000]$	$8.20 \pm 0.66 \pm 0.10$	-	-
R [Data]	$[2.000 - 3.700]$	$26.70 \pm 1.70 \pm 0.00$	-	-
J/ψ	$[3.088 - 3.106]$	$5.94 \pm 0.35 \pm 0.03$	-	-
$\psi(2S)$	$[3.658 - 3.714]$	$1.50 \pm 0.14 \pm 0.00$	-	-
R [Data]	$[3.700 - 5.000]$	$7.22 \pm 0.28 \pm 0.00$	-	-
R_{udsc} [QCD]	$[5.000 - 9.300]$	$6.87 \pm 0.10 \pm 0.00$	-	-
R_{udscb} [QCD]	$[9.300 - 12.00]$	$1.21 \pm 0.05 \pm 0.00$	-	-
R_{udscbt} [QCD]	$[12.0 - \infty]$	$1.80 \pm 0.01 \pm 0.00$	-	-
$\sum (e^+e^- \rightarrow \text{hadrons})$	$[2m_{\pi^\pm} - \infty]$	$684.7 \pm 6.0_{\text{exp}} \pm 3.6_{\text{rad}}$	$709.0 \pm 5.1_{\text{exp}} \pm 1.2_{\text{rad}} \pm 2.8_{\text{SU}(2)}$	$-24.3 \pm 7.9_{\text{tot}}$

¹ Not including ω and ϕ resonances (see text).

² Using isospin relations (see text).

³ e^+e^- data are used above 1.6 GeV (see text).

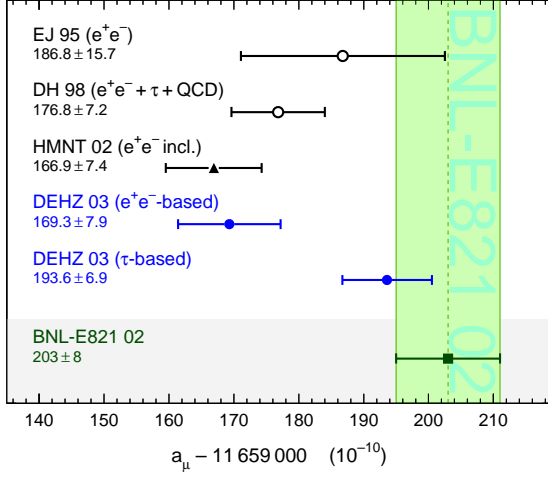


Figure 8. Comparison of the results with the BNL measurement [16]. Also shown are our previous estimates [3,11] obtained before the CMD-2 data were available, and the recent evaluation of Hagiwara *et al.* [52].

to facilitate the comparison with the data in the continuum. However, for the evaluation of the integral, the $b\bar{b}$ threshold is taken at twice the pole mass of the b quark, so that the contribution includes the narrow Υ resonances, according to global quark-hadron duality.

The contributions from the different processes in their indicated energy ranges are listed in Table 3. Wherever relevant, the two e^+e^- - and τ -based evaluations are given. The discrepancies discussed above are now expressed directly in terms of $a_\mu^{\text{had,LO}}$ giving smaller estimates for e^+e^- data by $(-21.2 \pm 6.4_{\text{exp}} \pm 2.4_{\text{rad}} \pm 2.6_{\text{SU(2)}} (\pm 7.3_{\text{total}})) 10^{-10}$ for the 2π channel and $(-3.1 \pm 2.6_{\text{exp}} \pm 0.3_{\text{rad}} \pm 1.0_{\text{SU(2)}} (\pm 2.9_{\text{total}})) 10^{-10}$ for the sum of the 4π channels. The total discrepancy $(-24.3 \pm 6.9_{\text{exp}} \pm 2.7_{\text{rad}} \pm 2.8_{\text{SU(2)}} (\pm 7.9_{\text{total}})) 10^{-10}$ amounts to 3.1 standard deviations and precludes from performing a straightforward combination of the two evaluations.

9.2. Results for a_μ

The results for the lowest order hadronic contribution are

$$a_\mu^{\text{had,LO}} = (684.7 \pm 6.0_{\text{exp}} \pm 3.6_{\text{rad}}) 10^{-10},$$

$$a_\mu^{\text{had,LO}} = (709.0 \pm 5.1_{\text{exp}} \pm 3.0_{\text{rad,SU(2)}}) 10^{-10},$$

where the first numbers are e^+e^- -based and the second τ -based. Adding the QED, higher-order hadronic, light-by-light scattering and weak contributions as given in Section 2, we obtain for a_μ

$$a_\mu^{\text{SM}} = (11\,659\,169.3 \pm 7.0_{\text{had}} \pm 3.5_{\text{LBL}} \pm 0.4_{\text{QED+EW}}) 10^{-10},$$

$$a_\mu^{\text{SM}} = (11\,659\,193.6 \pm 5.9_{\text{had}} \pm 3.5_{\text{LBL}} \pm 0.4_{\text{QED+EW}}) 10^{-10},$$

where again the first results are e^+e^- -based and the second τ -based. These values can be compared to the present experimental average given in Eq. (2). Adding experimental and theoretical errors in quadrature, the differences between measured and computed values are found to be (first number e^+e^- -based and the second τ -based)

$$a_\mu^{\text{exp}} - a_\mu^{\text{SM}} = (33.7 \pm 11.2) 10^{-10},$$

$$a_\mu^{\text{exp}} - a_\mu^{\text{SM}} = (9.4 \pm 10.5) 10^{-10},$$

corresponding to 3.0 and 0.9 standard deviations, respectively. A graphical comparison of the results with the experimental value is given in Fig. 8. Also shown are our previous estimates [3,11] obtained before the CMD-2 and the new τ data were available (see discussion below), and the recent evaluation of Hagiwara *et al.* [52].

10. DISCUSSION

10.1. The Problem of the 2π Contribution

The significant discrepancy between the e^+e^- and τ evaluations of $a_\mu^{\text{had,LO}}$ is a matter of concern. The following changes in the dominant $\pi^+\pi^-$ contribution (all expressed in 10^{-10} units) are observed with respect to our earlier work [11]:

- the new CMD-2 data [23] produce a downward shift of the e^+e^- evaluation by 1.9 (well within errors from previous experiments),

- the new ALEPH data [25] increases the τ evaluation by 3.5,
- including the CLEO data in the τ evaluation slightly improves the precision, but further raises the central value by 4.0,
- although including the OPAL data has little effect on the overall precision, it also increases the result by 1.9,
- the new complete isospin symmetry-breaking correction, including the re-evaluation of the S_{EW} factor, increases the τ evaluation by 0.2.

In principle, the observed discrepancy for the 2π contribution, (-21.2 ± 7.3) , or $(-4.2 \pm 1.4)\%$ when expressed with respect to e^+e^- , could be caused by any (or the combination of several) of the following three effects which we examine in turn:

- **The normalization of e^+e^- data**

Here, as below, 'normalization' does not necessarily mean an overall factor, but refers to the absolute scale of the 'bare' cross section at each energy point. There is no cross check of this at the precision of the new CMD-2 analysis. The only test we can provide is to compute the e^+e^- integral using the experiments separately. Because of the limited energy range where the major experiments overlap, we choose to perform the integration in the range of \sqrt{s} from 610.5 to 820 MeV. The corresponding contributions are: 313.5 ± 3.1 for CMD-2, 321.8 ± 13.9 for OLYA, 320.8 ± 12.6 for CMD, and 323.9 ± 2.1 for the isospin-corrected τ data. No errors on radiative corrections and isospin breaking are included in the above results.

- **The normalization of τ data**

The situation is quite similar, as the evaluation is dominated by the ALEPH data. It is also possible to compare the results provided by each experiment separately, with the spectral functions normalized to the respective hadronic branching ratios. Leaving aside the region below 500 MeV where

a fit combining analyticity constraints is used, the contributions are: 460.1 ± 4.4 for ALEPH, 464.7 ± 9.3 for CLEO and 464.2 ± 8.1 for OPAL, where the common error on isospin breaking has been left out. The three values are consistent with each other and even the less precise values are not in good agreement with the e^+e^- estimate in this range, 440.8 ± 4.7 , not including the error on missing radiative corrections.

Apart from an overall normalization effect, differences could originate from the shape of the measured spectral functions. If all three spectral functions are normalized to the world average branching ratio (our final procedure), then the results for the contribution above 0.5 GeV become: 459.9 ± 3.6 for ALEPH, 465.4 ± 5.1 for CLEO and 464.5 ± 5.1 for OPAL, with a common error of ± 2.4 from the $\pi\pi^0$ and leptonic branching ratios and the uncertainty on isospin breaking left out. Again the results are consistent and their respective experimental errors give a better feeling of the relative impact of the measurements.

- **The isospin-breaking correction applied to τ data**

The basic components entering SU(2) breaking have been identified. The weak points before were the poor knowledge of the long-distance radiative corrections and the quantitative effect of loops. Both points have been addressed by the analysis of Ref. [31] showing that the effects are small and covered by the errors previously applied. The overall effect of the isospin-breaking corrections (including FSR) applied to the 2π τ data, expressed in relative terms, is $(-1.8 \pm 0.5)\%$. Its largest contribution (-2.3%) stems from the uncontroversial short-distance electroweak correction. Additional contributions must be identified to bridge the observed difference.

Thus we are unable at this point to identify the source of the discrepancy. More experimental and theoretical work is needed. On the ex-

perimental side, additional data is available from CMD-2, but not yet published. As an alternative, a promising approach using e^+e^- annihilation events with initial state radiation (ISR), as proposed in Ref. [54], allows a single experiment to cover simultaneously a broad energy range. Two experimental programs are underway at Frascati with KLOE [55] and at SLAC with BABAR [56]. The expected statistics are abundant, but it will be a challenge to reduce the systematic uncertainty at the level necessary to probe the CMD-2 results. As for τ 's, the attention is now focused on the forthcoming results from the B factories. Again, the quality of the analysis will be determined by the capability to control systematics rather than the already sufficient statistical accuracy. On the theory side, the computation of more precise and more complete radiative corrections both for e^+e^- cross sections and τ decays should be actively pursued.

Other points of discussions are pursued in Ref. [22].

10.2. Consequences for $\alpha(M_Z^2)$

In spite of the fact that the present analysis was focused on the theoretical prediction for the muon magnetic anomaly, it is possible to draw some conclusions relevant to the evaluation of the hadronic vacuum polarization correction to the fine structure constant at M_Z^2 . The problem found in the 2π spectral function is less important for $\Delta\alpha(M_Z^2)$ with respect to the total uncertainty, because the integral involved gives less weight to the low-energy region. The difference between the evaluations using the 2π , 4π and $2\pi 2\pi^0$ spectral functions from e^+e^- and τ data are found to be:

$$\Delta\alpha_{\text{had}}^{ee}(M_Z^2) - \Delta\alpha_{\text{had}}^{\tau}(M_Z^2) = (-2.8 \pm 0.8) 10^{-4}.$$

While this low-energy contribution shows a 3.5 standard deviation discrepancy (when adding the different errors in quadrature), it also exceeds the total uncertainty of $1.6 10^{-4}$ on $\Delta\alpha(M_Z^2)$ which was quoted in Ref. [11]. It is worth pointing out that such a shift produces a noticeable effect for the determination of the Higgs boson mass M_H in the global electroweak fit [57]. With the present input for the electroweak observables [53] from LEP, SLC and FNAL yielding central values for

M_H around 100 GeV, going from the e^+e^- to the τ -based evaluation induces a decrease of M_H by 16 GeV using all observables and by 20 GeV when only the most sensitive observable, $(\sin^2 \theta_W)_{\text{eff}}$, is used.

11. CONCLUSIONS

A new analysis of the lowest-order hadronic vacuum polarization contribution to the muon anomalous magnetic moment has been presented. It is based on the most recent high-precision experimental data from e^+e^- annihilation and τ decays in the $\pi\pi$ channel. Special attention was given to the problem of isospin symmetry breaking and the corresponding corrections to be applied to τ data. The main results of our analysis are the following:

- the new evaluation based solely on e^+e^- data is significantly lower than previous estimates and is in conflict with the experimental determination of a_μ by 3.0 standard deviations.
- the new precise evaluations of the dominant $\pi\pi$ contributions from e^+e^- annihilation and isospin-breaking corrected τ decays are not anymore in agreement with each other. A discussion has been presented for possible sources of the discrepancy which could not be resolved. This situation is a matter of great concern, as the τ -based prediction of a_μ is in better agreement with the experimental value, from which it deviates by non-significant 0.9 standard deviations.

More experimental and theoretical work is needed to lift the present uncertainty on whether or not new physics has been uncovered with the muon magnetic moment.

Acknowledgements

I am indebted to my colleagues M. Davier, S. Eidelman and Z. Zhang for the pleasant collaboration. The close collaboration with V. Cirigliano, G. Ecker and H. Neufeld is gratefully acknowledged. Discussions with F. Jegerlehner, J. H. Kühn, A. Pich, A. Stahl, A. Vainshtein

and especially W. Marciano are appreciated. We thank S. Menke for providing us with the OPAL spectral functions. Finally, many thanks to Abe Seiden and his team for the preparation of the Tau'02 workshop.

REFERENCES

1. N. Cabibbo and R. Gatto, *Phys. Rev. Lett.* **4** (1960) 313; *Phys. Rev.* **124** (1961) 1577; L.M. Brown and F. Calogero, *Phys. Rev.* **120** (1960) 653.
2. C. Bouchiat and L. Michel, *J. Phys. Radium* **22** (1961) 121.
3. S. Eidelman and F. Jegerlehner, *Z. Phys.* **C67** (1995) 585.
4. R. Alemany, M. Davier and A. Höcker, *Eur.Phys.J.* **C2** (1998) 123.
5. R. Barate *et al.*, (ALEPH Collaboration), *Z. Phys.* **C76** (1997) 15.
6. R. Barate *et al.*, (ALEPH Collaboration), *Eur. J. Phys.* **C4** (1998) 409.
7. M. Davier and A. Höcker, *Phys. Lett.* **B419** (1998) 419.
8. J. H. Kühn and M. Steinhauser, *Phys. Lett.* **B437** (1998) 425.
9. A.D. Martin and D. Zeppenfeld, *Phys. Lett.* **B345** (1995) 558.
10. S. Groote *et al.*, *Phys. Lett.* **B440** (1998) 375.
11. M. Davier and A. Höcker, *Phys. Lett.* **B435** (1998) 427.
12. J. Bailey *et al.*, *Phys. Lett.* **B68** (1977) 191. F.J.M. Farley and E. Picasso, "The muon ($g - 2$) Experiments", Advanced Series on Directions in High Energy Physics - Vol. 7 Quantum Electrodynamics, ed. T. Kinoshita, World Scientific 1990.
13. R.M. Carey *et al.* (Muon ($g - 2$) Collaboration), *Phys. Rev. Lett.* **82** (1999) 1632.
14. H.N. Brown *et al.* (Muon ($g - 2$) Collaboration), *Phys. Rev.* **D62**, (2000) 091101.
15. H.N. Brown *et al.* (Muon ($g - 2$) Collaboration), *Phys. Rev. Lett.* **86**, (2001) 2227.
16. G. W. Bennett *et al.* (Muon ($g - 2$) Collaboration), *Phys. Rev. Lett.* **89** (2002) 101804; Erratum-ibid. **89** (2002) 129903.
17. M. Hayakawa, T. Kinoshita and A.I. Sanda, *Phys. Rev.* **D54** (1996) 3137; M. Hayakawa, T. Kinoshita and A.I. Sanda, *Phys. Rev. Lett.* **75** (1995) 790.
18. J. Bijnens, E. Pallante and J. Prades, *Nucl. Phys.* **B474** (1996) 379.
19. M. Knecht *et al.*, *Phys.Rev.* **D65** (2002) 073034.
20. M. Hayakawa and T. Kinoshita, Erratum *Phys. Rev.* **D66** (2002) 019902; *ibid.* **D57** (1998) 465.
21. J. Bijnens, E. Pallante and J. Prades, *Nucl.Phys.* **B626** (2002) 410.
22. M. Davier, S. Eidelman, A. Höcker and Z. Zhang, LAL-02-81, hep-ph/0208177 (2002).
23. R.R. Akhmetshin *et al.* (CMD-2 Collaboration), *Phys.Lett.* **B527** (2002) 161.
24. J.Z.Bai *et al.* (BES Collaboration), *Phys. Rev. Lett.* **84** (2000) 594; *Phys. Rev. Lett.* **88** (2002) 101802.
25. ALEPH Collaboration, ALEPH 2002-030 CONF 2002-019, (July 2002).
26. S. Anderson *et al.* (CLEO Collaboration), *Phys.Rev.* **D61** (2000) 112002.
27. K. W. Edwards *et al.* (CLEO Collaboration), *Phys.Rev.* **D61** (2000) 072003.
28. K. Akerstaff *et al.* (OPAL Collaboration), *Eur. Phys. J.* **C7** (1999) 571.
29. H. Czyż and J. H. Kühn, *Eur.Phys.J.* **C18** (2001) 497.
30. V. Cirigliano, G. Ecker and H. Neufeld, *Phys. Lett.* **B513** (2001) 361.
31. V. Cirigliano, G. Ecker and H. Neufeld, *JHEP* **0208** (2002) 002.
32. V. W. Hughes and T. Kinoshita, *Rev. Mod. Phys.*, **71** (1999) S133.
33. A. Czarnecki and W.J. Marciano, *Nucl. Phys. (Proc. Sup.)* **B76** (1999) 245.
34. B. Krause, *Phys. Lett.* **B390** (1997) 392.
35. A. Czarnecki, W.J. Marciano and A. Vainshtein, hep-ph/0212229 (Dec. 2002); see also the earlier works: A. Czarnecki, B. Krause and W.J. Marciano, *Phys. Rev. Lett.* **76** (1995) 3267; *Phys. Rev.* **D52** (1995) 2619; R. Jackiw and S. Weinberg, *Phys. Rev.* **D5** (1972) 2473; S. Peris, M. Perrottet and E. de Rafael, *Phys. Lett.* **B355** (1995) 523; M. Knecht *et al.*, *JHEP* **0211** (2002) 003.
36. M. Gourdin and E. de Rafael, *Nucl. Phys.* **B10** (1969) 667.
37. S.J. Brodsky and E. de Rafael, *Phys. Rev.* **168** (1968) 1620.
38. R.R.Akhmetshin *et al.* (CMD-2 Collaboration), Preprint BudkerINP 1999-10, Novosibirsk (1999).
39. S.J. Dolinsky *et al.* (ND Collaboration), *Phys. Rep.* **C202** (1991) 99.
40. R.R.Akhmetshin *et al.* (CMD-2 Collaboration), *Phys. Lett.* **B466** (1999) 392.
41. M.N.Achasov *et al.* (SND Collaboration),

- Preprint BudkerINP 2001-34, Novosibirsk (2001).
42. D. Buskulic *et al.* (ALEPH Collaboration), *Z. Phys.* **C70** (1996) 579.
 43. P. Tsai, *Phys. Rev.* **D4** (1971) 2821.
 44. Review of Particle Physics, K.Hagiwara *et al.*, *Phys. Rev.* **D66** (2002) 010001.
 45. A. Höfer, J. Gluza and F. Jegerlehner, *Eur. Phys. J.* **C24** (2002) 51.
 46. W. Marciano and A. Sirlin, *Phys. Rev. Lett.* **61** (1988) 1815.
 47. M. Artuso *et al.* (CLEO Collaboration), *Phys. Rev. Lett.* **72** (1994) 3762.
 48. K. Ackerstaff *et al.* (OPAL Collaboration), *Eur. Phys. J.* **C4** (1998) 93.
 49. R. Barate *et al.* (ALEPH Collaboration), *Eur. Phys. J.* **C11** (1999) 599.
 50. M. Battle *et al.* (CLEO Collaboration), *Phys. Rev. Lett.* **73** (1994) 1079.
 51. S.R. Amendolia *et al.* (NA7 Collaboration), *Nucl. Phys.* **B277** (1986) 168.
 52. K. Hagiwara, A.D. Martin, D. Nomura and T. Teubner, KEK-TH-844, IPPP-02-52, DCPT-02-104, CERN-TH-2002-233, hep-ph/0209187 (2002);
T. Teubner, Talk given at ICHEP'02, Amsterdam, The Netherlands, 2002.
 53. LEP Electroweak Working Group, LEPEWWG/2002-01 (May 2002).
 54. S. Binner, J.H. Kühn and K. Melnikov, *Phys. Lett.* **B459** (1999) 279.
 55. G. Cataldi *et al.* (KLOE Collaboration), in *Physics and Detectors for DAPHNE* (1999) 569.
 56. E. P. Solodov (BABAR Collaboration), hep-ex/0107027 (2001).
 57. K. Hagiwara, S. Matsumoto, D. Haidt and C.S. Kim, *Z. Phys.* **C64** (1994) 559.